Monte Carlo Simulation for the Structure of Polyolefins Made with Two Metallocene Catalysts in a Batch Reactor

3 AUTHORS, INCLUDING:

Nathanael Inkson
CD-adapco

8 PUBLICATIONS **408** CITATIONS

Monte Carlo Simulation for the Structure of Polyolefins Made with Two Metallocene Catalysts in a Batch Reactor

Nathanael J. Inkson, Chinmay Das, and Daniel J. Read*

School of Mathematics, University of Leeds, Leeds, LS2 9JT, U.K.

Received March 23, 2006; Revised Manuscript Received May 10, 2006

ABSTRACT: The synthesis of polyolefins with two metallocene catalysts is explored via a simple Monte Carlo simulation in the two cases of a batch and a semibatch reactor. The algorithm we develop can be applied, in principle, to an arbitrary number of catalysts with different propensities toward the formation of long chain branches. We compare our model to an experimental two-catalyst system, in which one of the catalysts makes only linear chains and the ratio of the two catalysts is varied, to synthesize a series of different molar mass resins. Results from our simulations show good agreement with experimentally measured molecular weight distributions, the ratio of unsaturated to saturated chain ends (found by ^{13}C NMR) and the number of branches per 10000C. We also examine the effect on the amount of branching when molecular hydrogen gas is added to the system to act as a chain transfer agent.

1. Introduction

Metallocene-catalyzed polyolefins are of considerable industrial interest due to the amount of control over the molecular weight and branching distribution that they bring. It is well-known that small amounts of branching can have a considerable effect on the rheology and hence the processability of polymers. Constrained geometry catalysts (CGCs) and other metallocene catalysts have been widely used to produce polyethylene with long chain branches (LCB).[1,2] LCB formation has been observed in solution, gas, and slurry reactors. The generally accepted mechanism of branch formation is that chains terminated with unsaturated (usually vinyl) groups can be incorporated by the CGC into a growing chain in the place of an ethylene (ethene) molecule, creating a branch. These vinyl-terminated chains are known as macromonomers and can be formed at the catalyst site via β-hydride elimination or catalyst transfer to an ethylene molecule.

Single site metallocene-catalyzed linear polyolefins typically have molecular weight distributions with a value of M_w/M_N of approximately 2.0. This tends to make the polymer suffer flow instabilities under processing conditions. A second catalyst can broaden the molecular weight distribution, since chains formed at the second site will typically have a different average molar mass. A common strategy[3-5] is for the second catalyst to form only linear chains, but with a high propensity for the formation of macromonomers: this can potentially increase the amount of branching. The choice of the molecular weight of the macromonomers being made by each catalyst is crucial to determine the rheological properties as the presence of a few long arms exponentially increases relaxation times of branched polymer melts.[6] Theoretical methods for determining the branching distribution and chain connectivity are useful to aid the control of such reactions, and they are essential to the subsequent prediction of the rheology of dual metallocene-catalyzed polyolefins.

The statistics of metallocene-catalyzed polymers has been extensively studied in the case of the idealized continuous stirred tank reactor (CSTR) at steady state. Soares and Hamilec studied single site metallocene-catalyzed polymers and derived analytical expressions for molecular weight and long chain branching distributions.[7-9] This work was extended to characterize the branching architecture in terms of priority and seniority, statistical parameters relevant to rheological behavior.[10] Monte Carlo simulation, at the level of the monomer, has been used to determine detailed structure for single site metallocenes.[3,11] The synthesis of polyolefins with two metallocene catalysts in CSTR conditions has been studied by both Monte Carlo simulation at the monomer level[4,12,13] and analytically.[13-15] The combination of these two methods allows a full description of the distribution of molecular architectures in this idealized reaction situation. It is often the case, however, that lab-scale and pilot polymerizations are necessarily performed under batch or semibatch conditions. It is thus useful to be able to make predictions of molecular parameters under these conditions, both for the laboratory determination of catalyst reaction rate constants and for determining appropriate operating conditions to make new and potentially useful resins. It is also important to introduce new methods that have potential for application to reactors which cannot be classified according to the standard definition of a CSTR, such as reactors with stagnant zones, or temperature and concentration heterogeneities.

For batch and semibatch reactors, some analytical results for averaged quantities such as number-average molecular weight and branching density exist.[16] Iedema and Hoefsloot[17] proposed a scheme based on numerical solution of population balance equations to predict molecular weight distributions and mean branching levels. Neither of these approaches is able to give direct information on the topological connectivity of the chains formed. In this paper, we describe a Monte Carlo algorithm for generating a statistical sample of molecular architectures.

The algorithm is a modification of the "random sampling technique", described by Tobita,[18] and applied by him to free-radical polymerization to form low-density polyethylene[19,20] and poly(vinyl acetate).[21,22] In particular, our simulation method for long-chain branching via terminal double bond incorporation is equivalent to that used by Tobita for vinyl acetate polymerization.[21,22] In common with Tobita's algorithm, we distinguish the direction in which segments in the molecule were grown (termed "downstream" by Read and McLeish[10]) from the opposite direction ("upstream"). This distinction is necessary when evaluating the statistics of the molecular shape. Our algorithm differs most strongly from those of Tobita[18-22] in that

we do not assume our linear "primary chains" are created instantaneously in the reactor. Instead, we allow for the possibility that reactor conditions might vary during the finite time of creation of a single primary chain, giving rise to (for example) variations in branching density along it (see section 5).

Our algorithm differs from those commonly used for metallocene systems,[3,11−13] in that it generates molecular structures on a segment-by-segment rather than a monomer-by-monomer basis (although ref 11 does both), and in that it does not require the prior generation of a pool of sample "macromonomers" for incorporation into the current chain. It does this by making use of analytically derivable results at the segment level, paying particular attention to the direction of polymer growth. This means that the algorithm is orders of magnitude faster than monomer-based calculations and requires significantly lower memory because storage of a macromonomer pool is redundant, and there is no "start up time" to create representative macromonomers. Although we describe this algorithm for the batch and semibatch cases, a similar approach is applicable for the CSTR reaction and is described in ref 23 for the case of a single catalyst.

In what follows, we first present the details of the reaction we consider, and analytical expressions for the overall concentrations of various species in the reactor. We then present an analysis of a number of important statistics at the segment level, which will be used in our subsequent description of the Monte Carlo algorithm itself. We then compare the results of this model to published experimental data for a lab-scale synthesis of a dual catalyst polymer, in which the ratio of the two catalysts is systematically varied.[4,24] Specifically, we compare to the experimentally measured molecular weight distributions, the ratio of unsaturated to saturated chain ends and the number of branches per 10000C. Finally, we analyze the structures generated in terms of their seniority and priority statistics.
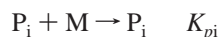
2. Reaction Chemistry

Our starting point is the polymerization reaction kinetics as described by Soares[14] but used throughout the relevant literature:[3−5,7−17]
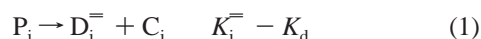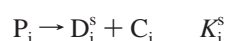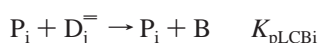
1. Initiation

$$C_i + M \rightarrow P_i \quad K_{pi}$$
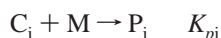
2. Monomer addition

$$P_i + M \rightarrow P_i \quad K_{pi}$$

3. Chain transfer to form a dead chain with unsaturated end

$$P_i \rightarrow D_i^= + C_i \quad K_i^= - K_d \quad (1)$$

$$P_i \rightarrow D_i^= + C_i^{deact} \quad K_d$$

4. Chain transfer to form a dead chain with saturated end

$$P_i \rightarrow D_i^s + C_i \quad K_i^s$$

5. Macromonomer (LCB) incorporation

$$P_i + D_j^= \rightarrow P_i + B \quad K_{pLCBi}$$

These reactions are written in terms of the total numbers of each object in the reactor (we deliberately avoid distinguishing between chains which possess different molecular weights or number of branches, as one would for a full population-balance

approach). The first two reactions represent initiation and growth of a polymer chain, where M is a monomer, C_i is an active but unattached catalyst of type i, and P_i is a living chain growing at a site of type i. As the catalysis proceeds the chain remains attached to the catalyst. In the third reaction the chain detaches from the catalyst leaving the chain terminated with a double bond, i.e., a macromonomer $D_i^=$. This process of double bond termination occurs by β-hydride elimination or by catalyst transfer to a monomer.[14] The chains terminated by double bonds can be reincorporated to a growing chain to form branches in the polymer structure. Reaction four occurs when the chain leaves the catalyst as before but without a terminal double bond, giving a saturated "dead chain" (D_i^s). Chain transfer agents such as hydrogen promote this reaction.

In the bulk of this paper, we have made the assumption that these two chain-transfer reactions obey first-order kinetics (i.e., with fixed rate constants during the reaction). For transfer to monomer or chain transfer agent, when the concentration of these species varies appreciably during the reaction, these equations will take on a (partially) second-order nature. Appendix C details how the equations developed in this paper are modified in such cases.

The final reaction is the reincorporation of a chain with a double bond at the end (vinyl terminated) into a growing chain, forming a long chain branch (B), which is, of course, part of the new chain, P_i. Although the branch is not strictly a separate chemical species, we use the (nonstandard) notation employed in reaction 5 to emphasize that branches are objects in the reactor which can be counted, and for which rate equations can be usefully written (see eq 13 below).

In batch and semibatch reactors, it is important to account for catalyst deactivation, which slows the rate of reaction as the polymerization proceeds. In the above scheme, we have made the assumption that deactivation occurs specifically at the third reaction: it must occur *somewhere* in the reaction scheme, but it is not particularly crucial where (one could, more conventionally, write the deactivation step as simply $C_i \rightarrow C_i^{deact}$, but the rate constant for this process would need to be of order $K_{pi}M/(K_i^= + K_i^S)$ faster than the average rate of catalyst deactivation, K_d, because of the low concentration of the unattached C_i relative to P_i). We make the further assumption that catalyst deactivation occurs at the same rate, K_d, for all the catalysts in the system. In what follows, this assumption allows the differential equations for overall concentrations in the reactor to be solved analytically. In the general case, one would need to resort to numerical solution of such equations within the overall Monte Carlo scheme. This complicates the algorithm we describe, without altering its overall structure; for clarity of presentation we restrict ourselves here to this simplest case. Fortunately, the approximation of uniform deactivation rate turns out to be a good one for the experiments we model in this paper,[24] where (see later) there is less than a 10% difference in measured deactivation rate between the two catalysts.

3. Concentrations in the Reactor and Dimensionless Quantities

In what follows, we denote the concentrations of reactor species using italic font, and retain Roman font for the species themselves. For example, P_i is the concentration of species P_i. We also denote the *total* concentration of active catalyst i as $Y_i = P_i + C_i$, and the total active catalyst concentration as

$$Y = \sum_i Y_i$$

Table 1. Dimensionless Variables

dimensionless deactivation rate	$k_d = \dfrac{K_d}{Y_0 \sum_j K_{pj}\phi_j}$
dimensionless rate of chain transfer to form a chain with unsaturated end for catalyst i	$k_i^{=} = \dfrac{K_i^{=}\phi_i}{Y_0 \sum_j K_{pj}\phi_j}$
dimensionless rate of chain transfer to form a dead chain with saturated end for catalyst i	$k_i^{s} = \dfrac{K_i^{s}\phi_i}{Y_0 \sum_j K_{pj}\phi_j}$
ratio of monomer and macromonomer polymerization rates for catalyst i	$q_{LCBi} = \dfrac{K_{pLCBi}}{K_{pi}}$
relative rate of monomer reaction due to catalyst i	$k_{pi} = \dfrac{K_{pi}\phi_i}{\sum_j K_{pj}\phi_j}$
dimensionless rate of macromonomer reaction	$r_{LCB} = \dfrac{\sum_i K_{pLCBi}\phi_i}{\sum_j K_{pj}\phi_j} = \sum_i k_{pi}q_{LCBi}$
dimensionless initial monomer concentration	$m_0 = \dfrac{M_0}{Y_0}$

which has an initial value Y_0. We write concentrations in nondimensional form as follows:

$$y = \frac{Y}{Y_0}, \quad y_i = \frac{Y_i}{Y_0}, \quad c_i = \frac{C_i}{Y_0}, \quad p_i = \frac{P_i}{Y_0}, \quad m = \frac{M}{Y_0}, \quad d_i^{=} = \frac{D_i^{=}}{Y_0},$$

$$d_i^{s} = \frac{D_i^{s}}{Y_0}, \quad b = \frac{B}{Y_0} \quad (2)$$

We also assume that the reactor conditions are such that $K_{pi}M \gg (K_i^{=} + K_i^{s})$ and $K_{pi}M \gg K_d$, in which case we are able to make a quasi-static approximation (see Appendix A) for the dynamics of the catalyst and living chain variables p_i and y_i. These variables are very well approximated by

$$p_i \approx y_i \approx \phi_i \exp(-K_d t) \quad (3)$$

where $\phi_i = Y_i/Y$ is the fraction of active catalyst i (since deactivation rates are the same for all catalysts, the ϕ_i values are time-independent).

It is convenient to define a set of dimensionless quantities, which determine the progress of the polymerization and, ultimately, the structures formed. These are listed in Table 1.

It is also convenient to define a dimensionless time variable, T, chosen by noting that the rate at which monomers react is proportional to $\sum_i K_{pi}Y_i$. We write

$$\frac{dT}{dt} = \sum_i K_{pi}Y_i = \frac{K_d}{k_d}\exp(-K_d t) \quad (4)$$

and hence

$$\exp(-K_d t) = 1 - k_d T \quad (5)$$

The dimensionless time, T, has a simple relationship with the monomer conversion, which we define as $x = M_R/M_0$ where

M_R is the concentration of reacted monomer and M_0 is the initial monomer concentration. We have

$$\frac{dx}{dT} = \frac{M}{M_0} \quad (6)$$

In a semibatch reactor, new monomer is added to keep the concentration of unreacted monomer constant, $M = M_0$, so this gives

$$x = T \quad \text{(for a semibatch reactor)} \quad (7)$$

In a batch reactor monomer is used up so that $M = M_0(1 - x)$ and so

$$x = 1 - \exp(-T) \quad \text{(for a batch reactor)} \quad (8)$$

In terms of these variables, the rate of change of concentration of macromonomers formed at catalyst i is

$$\frac{d[d_i^{=}]}{dT} = k_i^{=} - r_{LCB}d_i^{=} \quad (9)$$

and so

$$d_i^{=} = \frac{k_i^{=}}{r_{LCB}}[1 - \exp(-r_{LCB}T)] \quad (10)$$

Similarly, for the dead chains

$$\frac{d[d_i^{s}]}{dT} = k_i^{s} \quad (11)$$

and so

$$d_i^{s} = k_i^{s}T \quad (12)$$

The rate of change of total branch concentration is

$$\frac{db}{dT} = r_{LCB}\sum_i \bar{d_i^=} = \sum_i k_i^=(1 - \exp(-r_{LCB}T)) \quad (13)$$

which gives

$$b = \sum_i k_i^= \left(T - \frac{(1 - \exp(-r_{LCB}T))}{r_{LCB}}\right) \quad (14)$$

4. Statistics at the Chain Segment Level

To define chain-segment statistics, it is useful to know the rate of growth at a given catalyst site and to have information on the rate of branching and chain termination. Provided no other processes occur, the rate of monomer addition at a catalyst site i is

$$\frac{dN_i}{dt} = K_{pi}M \quad (15)$$

The rate of monomer addition with respect to the overall conversion, x, is

$$\frac{dN_i}{dx} = \frac{k_{pi}m_0}{\phi_i(1 - k_dT)} \quad (16)$$

It is convenient to define a normalized measure of degree of polymerization as $\tilde{N}_i = N_i/m_0$ so that the rate of increase of $\tilde{N}_i$ in the absence of other processes is

$$\frac{d\tilde{N}_i}{dx} = \frac{k_{pi}}{\phi_i(1 - k_dT)} \quad (17)$$

In practice, both chain termination and macromonomer incorporation occur, introducing chain ends and branch points, respectively. For a section of chain formed at conversion x, the mean distance to the nearest chain end in the direction of growth ("downstream") is found by comparing the relative rates of polymerization and termination, giving

$$\tilde{N}_{xi}^d = \frac{k_{pi}}{k_i^= + k_i^s}\frac{M}{M_0} \quad (18)$$

where $M/M_0 = 1$ for semibatch and $M/M_0 = (1 - x)$ for a batch reactor.

In the opposite ("upstream") direction, we compare the rates of initiation and chain growth. The rate of initiation is the same as the rate of termination, less the rate of catalyst deactivation. Hence, in the upstream direction, the mean distance to a chain end is

$$\tilde{N}_{xi}^u = \frac{k_{pi}}{(k_i^= + k_i^s - \phi_i k_d)}\frac{M}{M_0} \quad (19)$$

Similarly, the mean distance to the nearest branchpoint may be obtained by comparing the rates of monomer and macromonomer incorporation, giving

$$\tilde{N}_{bi} = \frac{M/M_0}{q_{LCBi}\sum_j \bar{d_j^=}} \quad (20)$$

where the quantity $\sum_j \bar{d_j^=}$ depends on the current time via eq 10. If a chain formed at a catalyst site i terminates, it could either form a macromonomer with probability

$$p^= = \frac{k_i^=}{(k_i^= + k_i^s)} \quad (21)$$

or a dead chain (with probability $p^s = k_i^s/(k_i^= + k_i^s)$). In the former case, there is a possibility that the macromonomer may at a later time be incorporated into another growing chain. Equation 9 indicates that the rate (with respect to the normalized time T) at which macromonomers are incorporated is given by the parameter r_{LCB}. Hence, the probability distribution of the time ΔT between macromonomer formation and reincorporation is

$$P(\Delta T) = r_{LCB} \exp(-r_{LCB}\Delta T) \quad (22)$$

In our algorithm, described below, a macromonomer formed at time T_1 is considered to be reincorporated at time $T_1 + \Delta T$ where ΔT is found from eq 22. If the re-incorporation time obtained is later than the time of the batch reaction, the macromonomer is still present in the final product of the reaction.

If a macromonomer is incorporated into a growing chain, then this chain could be attached to any of the catalysts that admit branches. The probability that it is incorporated into catalyst type i is found, from the relative rates of macromonomer incorporation into the different catalysts, as

$$\frac{q_i k_{pi}}{\sum_j q_j k_{pj}} \quad (23)$$

If a macromonomer is incorporated into the current chain at time T_1, forming a branch, then this macromonomer must have been formed at some time $T_2 < T_1$. The conditional probability distribution of T_2 given the current time T_1 is

$$P_{T1}(T_2) = \frac{r_{LCB} \exp(r_{LCB}T_2)}{\exp(r_{LCB}T_1) - 1} \quad (24)$$

The incorporated macromonomer could have been formed at any of the catalyst sites. The probability that it was formed at catalyst site i is

$$\frac{\bar{d_i^=}}{\sum_j \bar{d_j^=}} = \frac{k_i^=}{\sum_j k_j^=} \quad (25)$$

5. Monte Carlo Molecular Growth Algorithm

The algorithm we use follows the general methodology outlined by Tobita for free-radical polymerization[18−22] in that we build molecules by successively adding together linear chain segments, accounting for the above probabilities for side branches and chain termination. In contrast to Tobita, we allow for the possibility that, during the finite time between the initiation of primary chain and its termination by chain transfer, the batch reactor conditions may change. If this is the case, quantities such as branching density may vary along the chain length. We account for this by ensuring that the linear chain segments we add are always "short", in the sense that during the interval of conversion over which each such segment is polymerized, the change in reactor conditions is negligibly small. It may require several such short chain sections to make up a
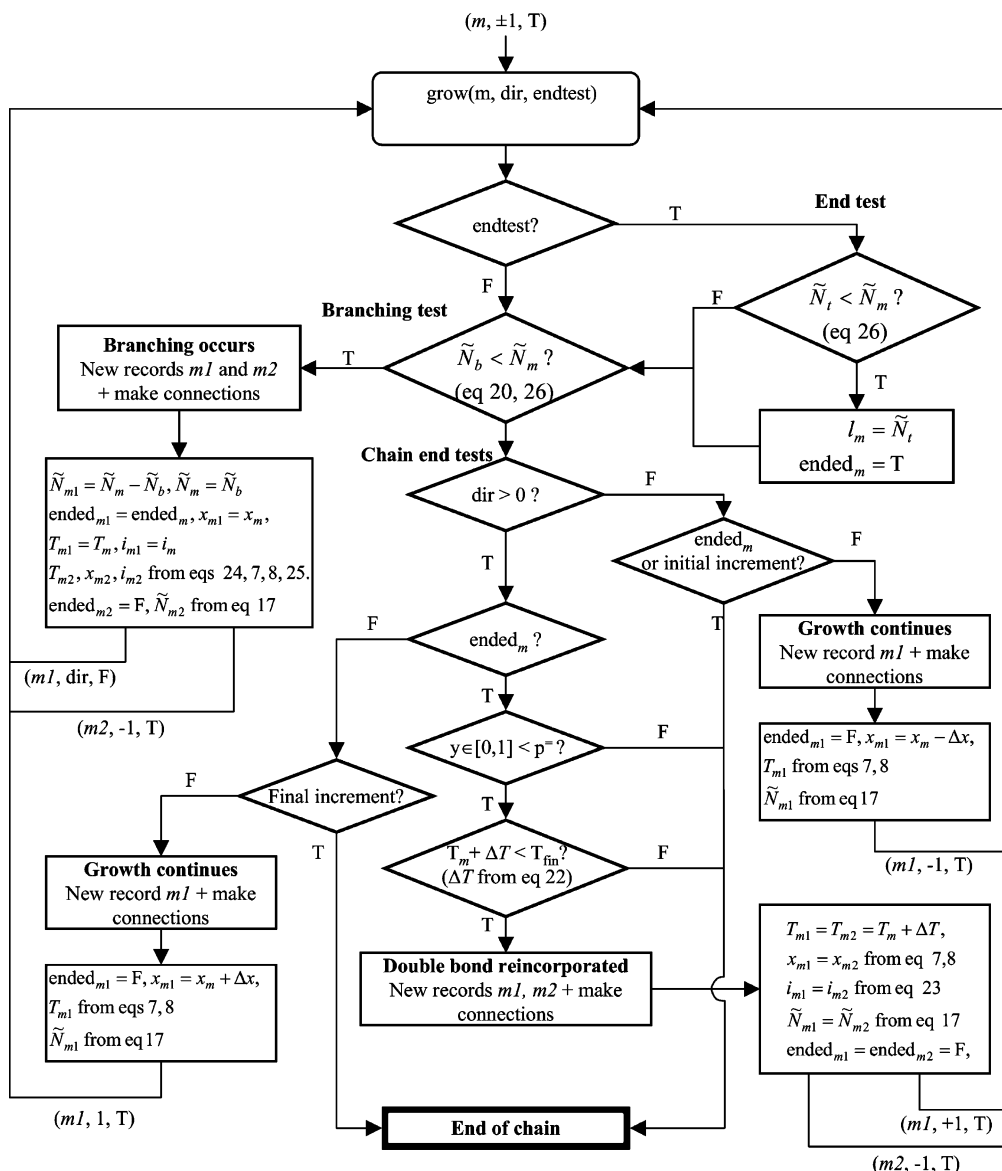
$(m, \pm1, \mathbf{T})$

grow(m, dir, endtest)

endtest?

End test

$\widetilde{N}_t < \widetilde{N}_m$?
(eq 26)

$l_m = \widetilde{N}_t$
ended$_m$ = T

Branching test

$\widetilde{N}_b < \widetilde{N}_m$?
(eq 20, 26)

Branching occurs
New records *m1* and *m2*
+ make connections

$\widetilde{N}_{m1} = \widetilde{N}_m - \widetilde{N}_b, \widetilde{N}_m = \widetilde{N}_b$
ended$_{m1}$ = ended$_m$, $x_{m1} = x_m$,
$T_{m1} = T_m, i_{m1} = i_m$
T_{m2}, x_{m2}, i_{m2} from eqs 24, 7, 8, 25.
ended$_{m2}$ = F, $\widetilde{N}_{m2}$ from eq 17

$(m1,$ dir, F$)$

$(m2, -1, \mathbf{T})$

Chain end tests

dir > 0 ?

ended$_m$
or initial increment?

Growth continues
New record *m1* + make connections

ended$_{m1}$ = F, $x_{m1} = x_m - \Delta x$,
T_{m1} from eqs 7, 8
$\widetilde{N}_{m1}$ from eq 17

$(m1, -1, \mathbf{T})$

ended$_m$?

$y \in [0,1] < p^=$?

Final increment?

Growth continues
New record *m1* + make connections

ended$_{m1}$ = F, $x_{m1} = x_m + \Delta x$,
T_{m1} from eqs 7, 8
$\widetilde{N}_{m1}$ from eq 17

$(m1, 1, \mathbf{T})$

$T_m + \Delta T < T_{\text{fin}}$?
(ΔT from eq 22)

Double bond reincorporated
New records *m1, m2* + make connections

$T_{m1} = T_{m2} = T_m + \Delta T,$
$x_{m1} = x_{m2}$ from eq 7,8
$i_{m1} = i_{m2}$ from eq 23
$\widetilde{N}_{m1} = \widetilde{N}_{m2}$ from eq 17
ended$_{m1}$ = ended$_{m2}$ = F,

$(m1, +1, \mathbf{T})$

$(m2, -1, \mathbf{T})$

End of chain

Figure 1. Flowchart of the recursive Monte Carlo algorithm for the growth of one polymer chain.

single primary chain. We know, from eq 17, that for a chain growing at catalyst site i, during an interval of conversion Δx (and provided the chain does not terminate), the normalized number of monomers added is $k_{pi}\Delta x/\phi_i(1 - k_d T)$. One of the inputs to the algorithm is a number, Δx_{max}, which is the maximum interval in conversion used for chain segments in the algorithm, chosen so that changes in (for example) macromonomer concentration are small over this interval. The choice of a very large value of Δx_{max} corresponds to the limit in which primary chains are considered to be created "instantaneously", as is done by Tobita for free-radical polymerization.[19−22]

At the heart of our Monte Carlo simulation is a recursive subroutine which, given an initial segment of chain being grown at a known value of conversion, *x*, will successively add extra chain segments and branches, incrementing the conversion appropriately. A flowchart for this subroutine is given in Figure 1. The fundamental steps which are repeated for each new segment of chain are as follows: (i) for a given interval of conversion Δx to add a segment of length $k_{pi}\Delta x/\phi_i(1 - k_d T)$ (i.e., the chain length assuming no termination occurs), then (ii) test to see whether the chain was, in fact, terminated during that interval and shorten the length appropriately, then (iii) test for branches along that chain section, then, finally, (iv) test for

other linked segment(s) at the end of the current chain segment. For computational convenience, step i is performed before the routine is called (i.e., the initial length of the subsegment is already set), and the routine begins with step ii. We now describe this routine, and these individual steps, in detail.

The routine requires that segments of chain are stored as records in the memory, each record being labeled with an integer *m*. Within each record is stored the length of the segment, the catalyst site on which it was grown, the time and conversion at which it was grown (assumed constant over a given segment), and two Boolean flags (one to indicate whether the segment is terminated during the reaction, and another to indicate whether the segment was formed right at the start of the batch reaction or right at the end). Finally, we store the connectivity of the molecule by storing the address of the connected segments to either side of the current chain segment (a maximum of two at either side, if both ends are branched).

On entry, the subroutine is provided with a chain segment (labeled with integer *m*) of known length, $\tilde{N}_m$, growing on known catalyst site, i$_m$, at a known value of the conversion x_m (which can be converted to reaction time *T* via eq 7 or 8 for semibatch and batch reactions respectively), in a known direction (upstream or downstream).

Once created, a section of chain must be tested to see whether the chain terminates along that section. This test should be performed once only on a given section of chain. It is possible to perform this test at the time of initial creation of the segment, but since there are several places in the routine at which new segments are created we find it computationally more convenient to place this test at the start of the routine and code for it once only. Whether this test is required is flagged via a Boolean variable on entry (when the subroutine is called for the first time for a given segment, this variable is set as true).

If this termination test is required, then we generate a random chain length $\tilde{N}_t$ from the Flory distribution

$$P_i(\tilde{N}_t) = \frac{1}{\tilde{N}_{xi}}\exp\left(-\frac{\tilde{N}_t}{\tilde{N}_{xi}}\right) \qquad (26)$$

where $\tilde{N}_{xi}$ is the mean distance to termination, given by eq 18 or 19 depending on the growth direction. If $\tilde{N}_t < \tilde{N}_m$, then termination occurs: the segment is marked as having terminated and the current segment length $\tilde{N}_m$ is set to $\tilde{N}_t$. For the downstream direction, the termination could either be to dead chain or macromonomer, but a decision on this is deferred until later.

Next, a decision is made on whether branches occur within the segment. For this, we generate a random length $\tilde{N}_b$ from a distribution of form (26), with mean $\tilde{N}_{bi}$ given by eq 20. If $\tilde{N}_b < \tilde{N}_m$ then the segment is branched at least once, and the first branch is a distance $\tilde{N}_b$ from the end of the segment. Two new segments, $m1$ and $m2$, are created. We set $\tilde{N}_{m1} = \tilde{N}_m - \tilde{N}_b$ and, subsequently, $\tilde{N}_m = \tilde{N}_b$ so that the original segment m is subdivided into new segments m and $m1$ either side of the branchpoint. Segment $m1$ inherits all other properties (including whether it is terminated or not) from segment m.

Segment $m2$ is the first segment of the incorporated side-branch. We obtain the time T_{m2} at which the corresponding macromonomer was formed from eq 24, and the catalyst type i_{m2} with probabilities given by eq 25. The length of this segment is initially set to $k_{pi}\Delta x_{max}/2\phi_i(1 - k_dT)$, corresponding to half the maximum increment.[25] The exception to this is when the conversion x_{m2} corresponding to T_{m2} is less than $\Delta x_{max}/2$, in which case this macromonomer was formed very near the start of the reaction. Its length is then set to $k_{pi}x_{m2}/\phi_i(1 - k_dT)$ and the segment is flagged as being formed within the first conversion increment.

Segments m, $m1$, and $m2$ are linked, by storing their addresses. The growth algorithm is called recursively for segments $m1$ and $m2$. $m1$ is grown in the same direction as segment m, and no termination test is required for this segment since it has already been performed on segment m. Segment $m2$ is grown in the upstream direction, with a flag that a termination test will be required for this segment.

Note that, since the routine is called recursively for segment $m1$, a further branching test is made on this segment. It is thus possible that, via repeated recursive calling of this routine, several branches will occur within the original segment m for which the routine was initially called. The probability distribution of the number of such branches follows a binomial distribution. In this sense, the addition of branches by this routine is equivalent to that of Tobita,[19-22] who calculates the total number of side branches on a given primary chain from such a binomial distribution.

In the absence of branching, the algorithm proceeds to the end of the current segment to decide what subsequent segments might be attached to it. Here the algorithm differs depending on whether the segment is being "grown" in the downstream or upstream direction.

For the downstream direction, if the segment is flagged as having terminated, then it will either terminate with a double bond (with probability $k_i^=/(k_i^= + k_i^s)$) or with a dead chain end. In the case of a double bond, the current segment forms a macromonomer, which might be reincorporated into another growing chain at some later time. To test for this, we generate a random time interval ΔT from the distribution in eq 22. If $T_{inc} = T_m + \Delta T$ is less than the final time of reaction for the batch process, then macromonomer reincorporation occurs at the time T_{inc}, giving a branch-point. The probability that the new branch is formed at a chain growing at catalyst i is given in eq 23.

Two new segments $m1$ (for growth upstream from the branchpoint) and $m2$ (for growth downstream from the branchpoint) are created, labeled as growing at time T_{inc}, with lengths obtained from $k_{pi}\Delta x_{max}/2\phi_i(1 - k_dT)$ evaluated at this time.[25] As above, an exception is made when the time T_{inc} lies within the initial or final increment of conversion for the batch process, in which case the length of (respectively) $m1$ or $m2$ is appropriately shorter, and the segment is labeled as such. Segments $m1$ or $m2$ are joined to each other and to m, to represent the branchpoint. The growth routine is called recursively for $m1$ or $m2$, in the upstream and downstream directions respectively, and with a flag requiring a termination test.

If the downstream segment is not terminated but was created within the final conversion increment of the batch reaction, then it would be expelled from the reactor still attached to the catalyst. We assume that this segment undergoes a termination process at some point afterward, and end the segment with a double bond or dead chain with the same probabilities as during the reaction.

If the segment is neither terminated, nor made within the final conversion increment, then growth of a linear chain continues at the end of the current segment. A new segment, $m1$, is created and attached to the current segment. $m1$ is grown at conversion $x_{m1} = x_m + \Delta x_{max}$ and has length $k_{pi}\Delta x_{max}/\phi_i(1 - k_dT)$ evaluated at this new conversion. Again, an appropriate exception is made when this puts segment $m1$ within the final conversion increment. The growth routine is called recursively for segment $m1$ in the downstream direction, with a flag for a termination test.

In the upstream direction, then either a chain termination or the segment being created within the initial conversion increment will result in an initiation site on the chain, and no further growth. Otherwise, growth of a linear chain continues at the end of the current segment. A new segment, $m1$, is created and dealt with in the same way as for downstream growth, but with conversion $x_{m1} = x_m - \Delta x_{max}$.

Hence, a single call to the above routine from an initial chain segment recursively grows that part of a branched molecule which is attached to the segment. To create a single branched molecule, we select a monomer at random from the polymers existing at the end of the batch reaction. This is equivalent to selecting a value of the conversion, x, uniformly between 0 and the final value of the conversion x_f. The probability that this monomer was reacted by catalyst i is

$$\frac{k_{pi}}{\sum_j k_{pj}} \qquad (27)$$

Having selected this monomer, we create and link together two chain segments, upstream and downstream from the randomly

Table 2. Reaction Variables Available from Ref 24

total reaction time, t_{fin}	600 s
measured propagation rate constant for Ind catalyst, K_{pInd}	740 L/(mol·s)
measured propagation rate constant for CGC catalyst, K_{pCGC}	370 L/(mol·s)
ind catalyst deactivation rate, $K_{d\ Ind}$	0.0056 s^{-1}
CGC catalyst deactivation rate, K_{dCGC}	0.0052 s^{-1}

selected monomer, each of length $k_{pi}\Delta x_{max}/2\phi_i(1 - k_d T)$ (unless the randomly chosen conversion is within $\Delta x_{max}/2$ of the beginning or end of the batch reaction, in which case one of the segments is shorter and flagged as being within one of these extreme conversion increments).[25] A call to the molecular growth routine, for each of these two segments, in the upstream and downstream directions respectively, results in the growth of an entire molecule.

Because the growth of a single molecule is initiated by selecting a monomer at random, the resulting distribution of molecules should be viewed as having been statistically chosen on a weight basis (i.e., the probability that a given molecule was grown is proportional to its weight, because larger molecules contain more monomers). This distribution can then be interrogated to obtain the statistics of any molecular parameters such as molecular weight, degree of branching, or the topological parameters of seniority and priority.

6. Comparison with Experimental Results

In this section we compare the results of our simulation with the experimental data published by Beigzadeh et al.[4] For these data, extra information on the reactor conditions can be found in Beigzadeh's thesis.[24] These data concern a set of semibatch reactions involving two catalysts, the metallocene Et[Ind]$_2$ZrCl$_2$ catalyst (which we shall refer to as Ind from hereon) and a constrained geometry catalyst (CGC), that allows the incorporation of macromonomers to create branching. In these reactions, the total monomer concentration was kept fixed at 0.9 mol/L and the total catalyst concentration, $Y = 4 \times 10^{-6}$ mol/L, but the ratio of the two catalysts was systematically varied. Reactions were carried out in the presence of varying quantities of H$_2$, which acts as a chain transfer agent (increasing the rate of termination to dead chain).

The other rate constants and reactor parameters available to us are listed in Table 2. For each catalyst, we do not have direct information on the parameters $K_i^=$ (rate of transfer to double bonds), K_i^s (rate of chain transfer to dead chain) and q_{LCBi} (ratio of monomer and macromonomer polymerization rates).

The measured data on the reaction product comprises of molecular weight distributions, the number of branches per 10000C and the ratio of unsaturated to saturated chain ends. Our algorithm is able to predict each of these quantities given a set of input parameters (additionally, the branches per 10000C and ratio of unsaturated to saturated chain ends can be evaluated analytically, as detailed in Appendix B, giving identical results to our algorithm). Our strategy for comparison is to use the measured data from the pure single catalyst systems to fix the parameters $K_i^=$, K_i^s and q_{LCBi} for each catalyst. We use the additional assumption that the parameters $K_i^=$ and q_{LCBi} do not vary with concentration of H$_2$ (i.e., having fixed $K_i^=$, K_i^s, and q_{LCBi} in the absence of H$_2$ we are allowed only to vary K_i^s when H$_2$ is introduced). Once the parameters are fixed for the pure catalyst reactions, there are no remaining free parameters for modeling the mixed catalyst systems; we must simply vary the ratio of the two catalysts in accordance with the experimental conditions.

Table 3. Parameter Sets for the Two Catalysts

catalyst	ind	CGC (model 1)	CGC (model 2)
K_i^s	0.09 s^{-1}	0.0072 s^{-1}	0.00 s^{-1}
$K_i^=$	0.94 s^{-1}	0.13 s^{-1}	0.19 s^{-1}
K_{pLCBi}/K_{pi}	0	6.5	8.5

We allowed ourselves one further liberty. We found that the predicted molecular weight distribution for the pure CGC catalyst was too narrow and did not agree with the GPC data. In other related work,[26] the breadth of the CGC molecular weight distribution was found to be widened with increasing concentrations in the amount of tris(pentafluorophenyl)borane cocatalyst (which also decreased the levels of long chain branching). This cocatalyst was used in the experiments we are presently considering. To account for the broadening of the molecular weight distribution, we modeled the CGC catalyst and cocatalyst system as a sum of two catalysts: CGC1 and CGC2, comprising fractions $(1 - f)$ and f of the total CGC concentration, respectively. These two catalysts possess differing polymerization rates, but otherwise identical reaction parameters. The combined propagation rate, $K_{pCGC} = (1 - f)K_{pCGC1} + f K_{pCGC2}$ is fixed to the known value for the CGC catalyst. For all of results reported, the resulting parametrization uses $f = 0.022$, $K_{pCGC1} = 330$ L/(mol·s) and $K_{pCGC2} = 2300$ L/(mol·s). Apart from broadening the predicted molecular weight distribution, this modification produces no appreciable effect on the following results.

For the following results, we performed Monte Carlo simulations using 10^6 molecules per run. The time required to evaluate molecular weight distributions for a given catalyst concentration is around 2 min (5 min for priority distributions) on a Pentium 4 processor. We used a conversion interval of $\Delta x_{max} = 0.005$ for all simulations and checked that this choice did not affect the repeatability of our results. We now consider finding the reaction parameters to give a good numerical model of the molecular weight distributions and the ratio of unsaturated to saturated chain ends, for the materials formed from the pure catalysts.

Table 3 lists the parameters obtained from fitting the GPC and NMR data for the pure catalyst systems. Two parameter sets are given for the CGC catalyst, one (model 1) which exactly matches the branching level and ratio of saturated to unsaturated chain ends, and a second (model 2) which explores the possibility of some error in the NMR measurements and allows the branching level to be slightly higher than measured for the pure CGC system. In both cases, the ratio of long chain branching reaction rate to rate of reaction to monomer (K_{pLCBi}/K_{pi}) is surprisingly high, yet it is required in order for the model to predict the observed levels of long chain branching. This feature has been discussed elsewhere by Nele and Soares,[16] although the ratio we use here appears to be even higher than suggested by them (they use a value of order 0.1). This discrepancy can, in part, be attributed to the fact that they did not include catalyst deactivation in their mathematical analysis (when we take the limit of no catalyst deactivation, the analytical results we derive in Appendix B are identical to those of ref 16, and then the present data can be fit with a ratio K_{pLCBi}/K_{pi} closer to 1).

Having matched the experimental data for the pure catalyst systems, we are then able to make predictions for the molecular weight distribution and NMR data for the mixed catalyst systems without further adjustable parameters. Figure 2 shows the comparison with the GPC data for models 1 and 2. We obtain a very good comparison with the molecular weight distributions for the individual pure catalyst cases. For the mixed catalyst systems, the computed molecular weight distributions are generally in excellent agreement with the GPC data, especially
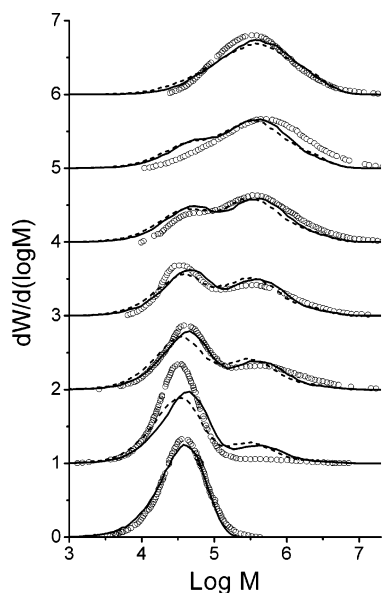
Figure 2. Experimental and computational molecular weight distributions for different ratios of the two catalysts. Curves are shifted vertically, for clarity, and represent (from bottom to top) 0% CGC, 20% CGC, 35% CGC, 50% CGC, 65% CGC, 80% CGC, and 100% CGC catalyst. The solid line gives the results from the "model 1" parameters, and the dashed line gives those from "model 2".
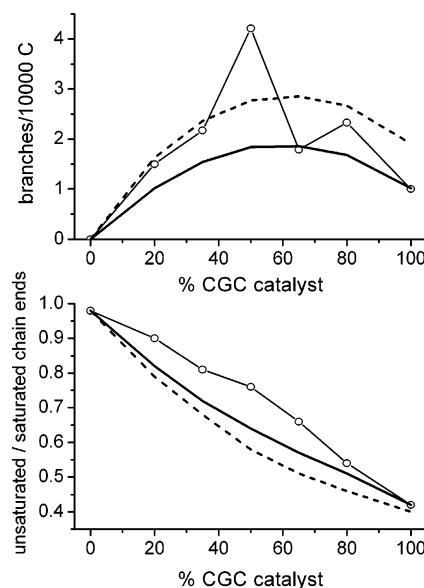

Figure 3. (Top) Number of branches per 10000C and (bottom) ratio of unsaturated to saturated chain ends, for the simulations using the reaction parameters of model 1 (solid line) and model 2 (dashed line), compared to the experimental data (circles).

considering that no fitting is being attempted here. For the case of 20% CGC we fail to predict the peak height of the molecular weight distribution and over-predict the high molecular weight fraction. We note that any model in which the 20% fraction of CGC catalyst is considered to behave ideally is bound to predict a substantial high molecular weight fraction in the way that we have, so this result is indicative of either some irregularity in the experimental conditions, or (perhaps) that the CGC catalyst is less active in low concentrations for some reason. One possibility (suggested by a referee of this work) is that the CGC catalyst is more sensitive to reactor impurities than the Ind catalyst; such selective poisoning would be most evident at low concentrations of the CGC catalyst.

Figure 3 compares the predicted number of branches per 10000C and ratio of saturated to unsaturated chain ends with the experimental NMR data for the full range of catalyst ratios. In the case of the branching levels, it can be seen that model 1 (which matches exactly the pure CGC value) seems to under-predict slightly the values for the mixed catalyst system. Nevertheless, the experimental data seem noisy, and it does not seem unreasonable to suggest that the experimental value for the pure CGC system might be too low. Model 2 explores this possibility by increasing the predicted value for the pure CGC case, and seems to lie better within the range of the experimental noise. Both models seem to match the overall trend in the data toward a peak in the level of branching at intermediate ratios of the two catalysts.

The ratio of saturated to unsaturated chain ends is reasonably well predicted, although the deviation from a linear mixing rule appears to be in the opposite sense to the experimental data.

We now consider the effect of adding hydrogen to the reactor on the resultant molecular weight distributions. For the CGC catalyst, this acts as a chain transfer agent, increasing the rate of chain transfer to dead chain (and so shifting the corresponding peak in the molecular weight distribution toward lower molecular weights). It appears to have little effect on the Ind catalyst. Here, we model the experimental data where 10 mL of H_2 was added to the reactor[4,21] simply by increasing the rate of chain

transfer to dead chain to $K_{CGC}^s = 0.17$ s^{-1} (for all other parameters, we took the values from model 2). Figure 4 demonstrates that the molecular weight distributions are again predicted with reasonable accuracy. The model predicts no change in the number of branches per 10000C when the parameter K_{CGC}^s is varied. Experimental results[4,24] indicate there might be a slight decrease in this quantity on the addition of H_2 (which could be attributed either to a decrease in the rate of macromonomer formation or the rate of macromonomer reincorporation). The decrease, however, appears to be slight, and may well be within the experimental scatter.

7. Analysis of Molecular Topologies

An advantage of the Monte Carlo method is that it permits immediate access to the molecular topologies that are predicted from a given reaction scheme. The physical properties of a polymer resin depend not only on the branching density but also on the placement of those branches within the polymer. One measure of the topology of molecules present in the resin, which has been used in the literature,[10,15] is to examine the statistical distribution of two quantities, *seniority* and *priority*. The seniority of a given polymer strand may be evaluated by counting the number of strands to the furthest free end in each chain direction (inclusive of the current strand, so the minimum seniority is 1). The strand seniority is then the smaller of the two values. The seniority is considered to be relevant to the rheological relaxation time of that strand. The priority of a given strand may be calculated by counting the number of free ends attached in each chain direction, then taking the smaller value from the two directions. The priority is related to the maximum stretch that a chain strand can achieve within the entanglement "tube", and is thought to be an important parameter when considering the limits of extension hardenning of the melt.

For a detailed discussion of how these parameters might be related to rheological models for the melt, we refer the reader to ref 10. Here we shall limit ourselves to an evaluation of the statistical distribution of these two quantities for the resins modeled here, which will give information on the variation of molecular topology with catalyst concentration.
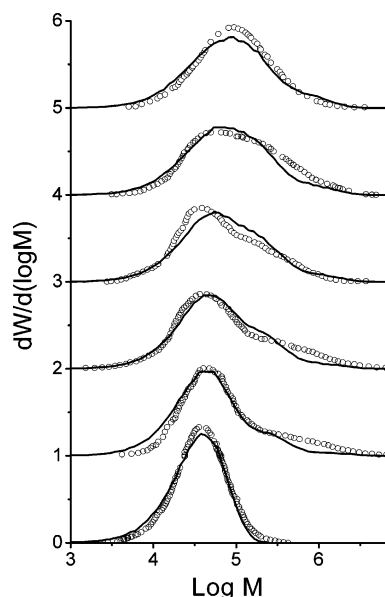
Figure 4. Experimental and computational molecular weight distributions for different ratios of the two catalysts, in the presence of hydrogen. Curves are shifted vertically, for clarity, and represent (from bottom to top) 0% CGC, 20% CGC, 35% CGC, 50% CGC, 65% CGC, and 80% CGC catalyst.
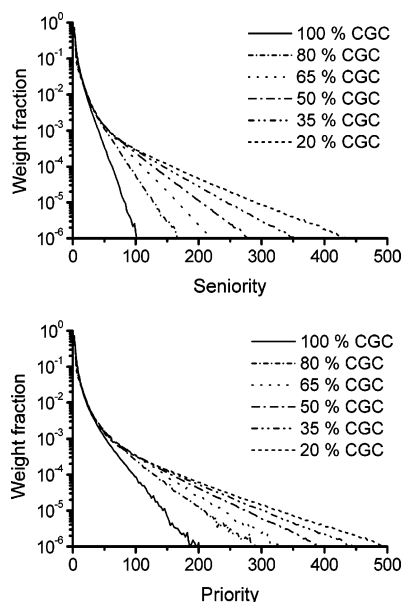

Figure 5. Distributions, by weight, of strands with given seniority (top) and priority (bottom) obtained for molecules computationally generated using the "model 2" parameters, at different ratios of the two catalysts.

Using the parameters that give the highest amount of branching (model 2), we used the molecules generated from our Monte Carlo algorithm to obtain the probability distribution that a strand, selected on a weight basis, would have a given value priority and seniority. The priority and seniority distributions, for each ratio of catalyst concentration, are shown in Figure 5. Two observations seem pertinent. First, it appears that the amount of material with the highest values of seniority and priority seems to increase monotonically with increasing concentration of the linear "Ind" catalyst (this is despite the fact that the number of branches per 10000C is a nonmonotonic function, as shown in Figure 3). Second, it appears that at the highest values of "Ind" catalyst concentration, the distributions of seniority and priority are very similar in shape, suggesting
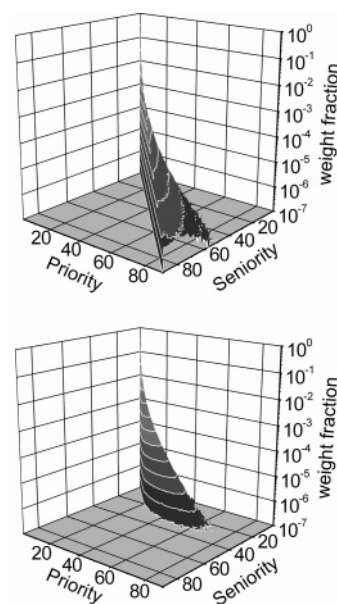

Figure 6. Calculated bivariate priority and seniority distribution for (top) the 20% CGC catalyst resin, and (bottom) 100% CGC catalyst resin

that the priority and seniority of a given segment should have a similar numerical value. This is confirmed in Figure 6, which shows the joint distributions of seniority and priority for both the 100% and 20% CGC systems. In the latter case, the distribution is very much biased toward the line where seniority and priority are equal (it is impossible for seniority to be greater than priority), whereas for the 100% CGC system, this line is not approached so closely and, typically, the priority of a segment is somewhat larger than its seniority when the values of both are large.

We may interpret these observations in terms of the typical structures of the molecules present in the resin. The only molecular topology for which the seniority is, for all strands, equal to the priority is the comb molecule. The above observations suggest that, while most of the 20% CGC resin consists of linear molecules formed at the Ind catalyst site, the majority of the remaining branched material comprises molecules which are largely comblike. Any branch-on-branch structures are formed from the joining together of comblike structures. From the chemical kinetics, it is easy to understand why the branched material is predominantly comblike in this case. If we consider a single polymer chain growing on a CGC site, we can compare the rates of branch incorporation and the rates of termination, which are

$$\text{rate of branching} = K_{pLCB}\overline{\overline{D}} = q_{LCB}K_p Y_0 \overline{\overline{d}}$$

$$\text{rate of termination} = K^s + K^{\overline{\overline{}}}$$

The ratio of these two quantities gives the typical number of branches that occur on a given growing chain before termination occurs. For the 20% CGC resin, and using the same parameters as above, this ratio approaches a value of just over 7 toward the end of the reaction, i.e., each chain growing on a CGC site obtains 7 branches, on average. Most of these branches occur by the incorporation of linear macromonomers formed at an Ind catalyst site (more than 95% of the macromonomers are formed at the Ind site), giving rise to the comblike structure.

A similar calculation for the 100% CGC resin indicates that the average number of branches occurring on a given growing chain before termination occurs is just less than 1 (0.9) at the

end of the reaction. In this case, however, all macromonomers are formed at the CGC site, and so there is a greater propensity toward branch-on-branch structures, giving rise to values of strand priority that substantially exceed the seniority, as is reflected in Figures 5 and 6.

While the 20% CGC resin contains mostly linear molecules, the higher rate of branching at the CGC site means the branched molecules in the 20% CGC resin typically contain many more branches than those in the 100% CGC resin, and thus contain strands with larger values of seniority and priority. This explains the monotonic increase of high priority and seniority material with Ind catalyst concentration reported in Figure 5.

8. Conclusions

We have presented a Monte Carlo algorithm for the simulation of molecular structures arising from polymerization of olefins using mixed metallocene catalysts in batch or semibatch reactors. The algorithm gives a computationally efficient solution to this problem, since it builds molecules on a strand-by-strand, rather than monomer-by-monomer basis. It provides an exact solution, provided the reaction mechanism and kinetics given in eq 1 are correct. Comparison with experimental results can therefore be taken as a direct test of this reaction mechanism.

We compared our model to an experimental two-catalyst system, in which one of the catalysts makes only linear chains and the ratio of the two catalysts is varied, to synthesize a series of different molar mass resins. Results from our simulations show good agreement with experimentally measured molecular weight distributions, the ratio of unsaturated to saturated chain ends (found by ^{13}C NMR) and the number of branches per 10000C. In particular, fixing the model parameters from the single catalyst systems provided sufficient information for reasonable prediction of available experimental data for all mixtures of the two catalysts, both with and without the addition of hydrogen as a chain transfer agent.

Several observations, however, indicate that the catalysts may not be behaving in the ideal fashion indicated in the commonly accepted reaction scheme of eq 1. The most serious indicator is the exceptionally large ratio of polymerization rates for long chain branching and monomer incorporation. Other, perhaps less significant, indicators include the breadth of the molecular weight distribution for the constrained geometry catalyst (which required the CGC catalyst to be modeled as a superposition of two "ideal" catalysts), and some deviations between the predicted and measured data (e.g., at small values of CGC catalyst concentration, the amount of high molecular weight material was over-predicted). Nele and Soares[16] have previously noted some of these issues, and proposed some possible reasons for the apparently high long chain branching rate constant. One possible explanation is that the macromonomers somehow attain a concentration around the catalyst sites, which is higher than the average value in the reactor. Nele and Soares suggested this might be due to slow diffusion of macromonomers away from the CGC catalyst site, but we note that this diffusion-based mechanism does not explain the high rate of incorporation, at the CGC sites, of macromonomers formed elsewhere at the Ind catalyst sites. One speculative alternative is that there may be some "clusters" of growing macromolecules, phase-separated from the reactor mixture, but containing both Ind and CGC catalyst sites at high local concentration.

It is through the development of models such as this one that such ideas can be tested. We have focused on the ideal reaction scheme and conditions, as presented in eq 1, where the differential equations for overall concentrations of various

species in the reactor could be solved analytically. The methodology presented here can, nevertheless, be extended toward nonideal reaction conditions, or more complicated reaction schemes, where the population balance equations would have to be solved numerically before being coupled to the Monte Carlo algorithm. Such an approach becomes necessary even after small modifications to the above reaction scheme (e.g., when catalyst deactivation rates differ appreciably). It is thus likely that, in modeling most reactions, numerical solution of the differential equations would be the required method.

Appendix A: Quasi-static Approximation for Catalyst Concentrations

We consider the rate equations for the concentrations of catalyst and living chain species. The concentration of unattached catalyst changes with time as

$$\frac{dc_i}{dt} = (K_i^= - K_d + K_i^S)p_i - K_{pi}Mc_i \tag{28}$$

where the suffix denotes the catalyst number. The living chain species have the following rate equation

$$\frac{dp_i}{dt} = K_{pi}Mc_i - (K_i^= + K_i^S)p_i \tag{29}$$

Changing variable from c_i to y_i in these equations gives

$$\frac{dy_i}{dt} = -K_d p_i \tag{30}$$

$$\frac{dp_i}{dt} = K_{pi}M(y_i - p_i) - (K_i^= + K_i^S)p_i \tag{31}$$

Polymerizations are generally carried out in the limit $K_{pi}M \gg (K_i^= + K_i^S)$ and $K_{pi}M \gg K_d$ in which case the solution of the above two equations is given by a very rapid relaxation of p_i toward y_i (on time scale $(K_{pi}M)^{-1}$) together with a slow decay of both variables toward zero (on time scale K_d^{-1}). Hence, these variables are very well approximated by

$$p_i \approx y_i \approx \phi_i \exp(-K_d t) \tag{32}$$

where $\phi_i = Y_i/Y$ is the fraction of catalyst i.

Appendix B: Analytical Results for the Degree of Branching and Ratio of Saturated to Unsaturated Chain Ends

The normalized branch concentration upon integration is given in eq 14, while the normalized concentration of reacted monomers is simply $m_0 x$. Since each monomer contains two carbons, the number of branches per 10000C is given by

$$\text{branches per } 10000\,C = \sum_i k_i^= \left(T - \frac{(1 - \exp(-r_{LCB}T))}{r_{LCB}}\right)\frac{5000}{m_0 x} \tag{33}$$

The normalized total polymer concentration, p_T is found by summing over all dead chains and living chains (which decay with time due to catalyst deactivation):

$$p_T = \sum_i (d_i^= + d_i^s) + \exp(-K_d t) \tag{34}$$

Using eqs 5, 10, and 12 in terms of dimensionless time, we find that

$$p_T = 1 - k_d T + \sum_i k_i^= \frac{(1 - \exp(-r_{LCB} T))}{r_{LCB}} + \sum_i k_i^s T \tag{35}$$

At the end of the reaction we assume that a fraction $k_i^= /(k_i^= + k_i^s)$ of the remaining living chains on catalyst i are terminated with a double bond, and the rest become saturated chain ends. Hence, the total number of unsaturated ends is

$$e_{unsat} = \sum_i \left[d_i^= + \frac{\phi_i k_i^=}{(k_i^= + k_i^s)}(1 - k_d T) \right] \tag{36}$$

On any given chain, the total number of chain ends is equal to the number of branch points plus 2. Therefore, the total number of ends for all chains ending with saturated or unsaturated groups is given by

$$e_{sat} + e_{unsat} = b + 2p_T \tag{37}$$

where the density of branch points, b is given in eq 14. Therefore, the ratio of saturated to unsaturated ends is simply

$$\frac{e_{unsat}}{e_{sat}} = \frac{e_{unsat}}{b + 2p_T - e_{unsat}} \tag{38}$$

Appendix C: Partially Second-Order Rate Kinetics for Chain-Transfer Reactions

In the bulk of this paper, we have made the assumption that the two chain-transfer reactions obey first-order kinetics (i.e., with fixed rate constants during the reaction). This assumption is incorrect in batch processes, for transfer to monomer or chain transfer agent, when the concentration of these species varies appreciably during the reaction. In such cases, it is reasonable to assume that the relevant rate constants vary linearly with conversion, x, and can be parametrized as

$$K_i^= = K_{0i}^= + K_{1i}^= (1 - x) \tag{39}$$

$$K_i^s = K_{0i}^s + K_{1i}^s (1 - x) \tag{40}$$

where the specific form has been chosen by noting that the monomer concentration in a batch reactor varies as $(1 - x)$. The dimensionless rate constants (Table 1) then vary in a similar way, as

$$k_i^= = k_{0i}^= + k_{1i}^= \exp(-T) \tag{41}$$

$$k_i^s = k_{0i}^s + k_{1i}^s \exp(-T) \tag{42}$$

where we have used eq 8. These two equations can be used directly in eqns 18, 19, and 21. They additionally give rise to different time variations for the concentrations of species in the reactor. Substituting into eq 9 and integrating gives

$$d_i^= = \frac{k_{0i}^=}{r_{LCB}}[1 - \exp(-r_{LCB} T)] +$$
$$\frac{k_{1i}^=}{r_{LCB} - 1}[\exp(-T) - \exp(-r_{LCB} T)] \tag{43}$$

which can be used in eq 20. Similarly, substituting into eq 11 and integrating gives

$$d_i^s = k_{0i}^s T + k_{1i}^s[1 - \exp(-T)] \tag{44}$$

Subsequent substitution into the rate of branch formation (eq 13) and integrating gives

$$b = \sum_i \left\{ k_{0i}^= \left(T - \frac{(1 - \exp(-r_{LCB} T))}{r_{LCB}} \right) + \frac{r_{LCB} k_{1i}^=}{r_{LCB} - 1} \left(1 - \exp(-T) - \frac{(1 - \exp(-r_{LCB} T))}{r_{LCB}} \right) \right\} \tag{45}$$

Finally, the statistics of macromonomer incorporation, in eqns 24 and 25, need modification. At time T_1, the total concentration of macromonomers is given by

$$d^= = \sum_i \frac{k_{0i}^=}{r_{LCB}}[1 - \exp(-r_{LCB} T_1)] + \frac{k_{1i}^=}{r_{LCB} - 1}[\exp(-T_1) - \exp(-r_{LCB} T_1)]$$

while the concentration of such chains that were formed within a small interval dT_2 at time $T_2 < T_1$ is given by

$$\sum_i [k_{0i}^= + k_{1i}^= \exp(-T_2)] \exp(-r_{LCB}(T_1 - T_2)) \, dT_2$$

The ratio of these two quantities gives the equivalent of eq 24, the conditional probability for the time, T_2, of creation of a macromonomer incorporated into a chain growing at time T_1:

$$P_{T1}(T_2) = \frac{\sum_i [k_{0i}^= + k_{1i}^= \exp(-T_2)] \exp(-r_{LCB}(T_1 - T_2))}{\sum_i \frac{k_{0i}^=}{r_{LCB}}[1 - \exp(-r_{LCB} T_1)] + \frac{k_{1i}^=}{r_{LCB} - 1}[\exp(-T_1) - \exp(-r_{LCB} T_1)]} \tag{46}$$

The probability that the incorporated macromonomer was formed at site i is

$$\frac{k_{0i}^= + k_{1i}^= \exp(-T_2)}{\sum_j [k_{0j}^= + k_{1j}^= \exp(-T_2)]} \tag{47}$$

References and Notes

(1) Lai, S. Y.; Wilson, J. R.; Knight, G. W.; Stevens, J. C.; Chum, P. W. S. US Patent 5,272,236 (Dow Chemical), 1993.
(2) Lai, S. Y.; Wilson, J. R.; Knight, G. W.; Stevens, J. C.; US Patent 5,665,800 (Dow Chemical), 1997.

(3) Beigzadeh, D.; Soares, J. B. P.; Duever, T. A.; Hamielec, A. E. *Polym. React. Eng.* **1999**, *7*, 195−205.

(4) Beigzadeh, D.; Soares, J. B. P.; Duever, T. A *Macromol. Rapid Commun.* **1999**, *20*, 541−545.

(5) Beigzadeh, D.; Soares, J. B. P.; Duever, T. A. *Macromol. Symp.* **2001**, *173*, 179−194.

(6) McLeish, T. C. B. *Adv. Phys.* **2002**, *51*, 1379−1527.

(7) Soares, J. B. P.; Hamielec, A. E. *Polymer* **1995**, *36*, 2257−2263.

(8) Soares, J. B. P.; Hamielec, A. E. *Macromol. Theory Simul.* **1996**, *5*, 547−572.

(9) Soares, J. B. P.; Hamielec, A. E. *Macromol. Theory Simul.* **1997**, *6*, 591−596.

(10) Read, D. J.; McLeish, T. C. B. *Macromolecules* **2001**, *34*, 1928−1945.

(11) Costeux, S.; Wood-Adams, P.; Beigzadeh, D. *Macromolecules* **2002**, *35*, 2514−2528.

(12) Simon, L. C.; Soares, J. B. P. *Macromol. Theory Simul.* **2002**, *11*, 222−232.

(13) Costeux, S. *Macromolecules* **2003**, *36*, 4168−4187.

(14) Soares, J. B. P. *Macromol. Theory Simul.* **2002**, *11*, 184−198.

(15) Read, D. J.; Soares, J. B. P. *Macromolecules* **2003**, *36*, 10037−10051.

(16) Nele, M.; Soares, J. B. P. *Macromol. Theory Simul.* **2002**, *11*, 939−943.

(17) Iedema, P. D.; Hoefsloot, H. C. J. *Macromolecules* **2003**, *36*, 6632−6644.

(18) Tobita, H. *Macromol. Theory. Simul.* **1996**, *5*, 1167−1194.

(19) Tobita, H. *J. Polym. Sci., Part B: Polym. Phys.* **2001**, *39*, 391−403.

(20) Tobita, H. *J. Polym. Sci., Part B: Polym. Phys.* **2001**, *39*, 2960−2968.

(21) Tobita, H. *J. Polym. Sci., Part B: Polym. Phys.* **1994**, *32*, 901−910.

(22) Tobita, H. *J. Polym. Sci., Part B: Polym. Phys.* **1994**, *32*, 911−919.

(23) Das, C.; Inkson, N. J.; Read, D. J.; Kelmanson, M. A.; McLeish, T. C. B. *J. Rheol.* **2006**, *50*, 207−235.

(24) Beigzadeh, D. Ph.D. Thesis. Institute for Polymer research, University of Waterloo, Waterloo, Ontario, N2L 3G1, Canada.

(25) The choice of a factor of 2 here is not essential to the running of the algorithm, but is not without justification. The algorithm is a "finite difference" algorithm, in which the value of "conversion" attributed to a given chain segment is the average value over that segment (or, in some sense, the value at the middle of the segment). Sometimes (e.g. at branchpoints) the routine calculates an "exact" value of the conversion right at a chain end, using eq 22 or eq 26. In this case, it is appropriate initially to take only a half-increment from the chain end, so that the chain end (where the "exact" conversion is known) lies halfway along a full increment.

(26) Beigzadeh, D.; Soares, J. B. P.; Duever, T. A. *J. Polym. Sci., Part A* **2004**, *42*, 3055−3061.